Cold-to-electricity conversion using a piston based engine in cold energy storage (CES) system, part one

Du, Yanping; Ding, Yulong

DOI:
10.1016/j.joei.2016.07.011

Document Version
Peer reviewed version

Citation for published version (Harvard):
Du, Y & Ding, Y 2016, 'Cold-to-electricity conversion using a piston based engine in cold energy storage (CES) system, part one: a theoretical study', *Journal of the Energy Institute*. https://doi.org/10.1016/j.joei.2016.07.011

Accepted Manuscript

Cold-to-electricity conversion using a piston based engine in cold energy storage (CES) system, part one: a theoretical study

Y.P. Du, Y.L. Ding

PII: S1743-9671(16)30184-2

DOI: 10.1016/j.joei.2016.07.011

Reference: JOEI 255

To appear in: *Journal of the Energy Institute*

Received Date: 8 April 2016

Revised Date: 24 July 2016

Accepted Date: 28 July 2016

Please cite this article as: Y.P. Du, Y.L. Ding, Cold-to-electricity conversion using a piston based engine in cold energy storage (CES) system, part one: a theoretical study, *Journal of the Energy Institute* (2016), doi: 10.1016/j.joei.2016.07.011.

Cold-to-electricity conversion using a piston based engine in cold energy storage (CES) system, part one: a theoretical study

Y.P. Du[1,*], and Y.L. Ding[2]

[1] *School of Chemical and Process Engineering, University of Leeds, LS2 9JT, UK*

[2] *School of Chemical Engineering, University of Birmingham, Edgbaston, Birmingham, B15 2TT, UK*

*Corresponding Author, email: Yanping.Du@csiro.au

Abstract: This study concerns the cold-to-electricity conversion in a piston based engine. A theoretical model was developed to predict the power generation rate in the engine. Parametric study showed the significant effect of p-crank angle, motor speed, gas pressure and temperature and chamber volume on the power generation by the piston based engine. It was found that optimal p-crank angle was normally in the range of 55^{o}~76^{o}. The minimum inner diameter of the valves connected to the engine was a crucial factor that limited the power capacity of the engine system. Based on the experimental data, the large engine (1900 cm^3) and small engine (162 cm^3) had an actual efficiency of 24.1% and -23.6%, respectively. This implied that the large engine was feasible to be used in CES system for electricity re-generation during peak hours. However, the induced CES efficiency was 18.9% and 52.1% in two different situations. The results indicate the importance of engine development in promoting the CES technology.

Keywords: Cold-to-electricity conversion; Piston based engine; Power generation rate; Engine efficiency; CES efficiency.

1. Introduction

Cold energy storage has attracted more and more attention due to its significant role in addressing the main energy challenges [1-2]. The CES technology is competitive in dealing with fluctuation of electricity demand (demand side) [3-4] and intermittency of renewable resources (supply side) [5-6]. Furthermore, the CES using cryogens as the storage media could achieve an exergy efficiency of over 80%, which enables the CES system competitive compared with thermal energy storage (TES) technologies in the energy discharging process [7].

As the essential component for cold-to-power conversion in a CES system, engine systems were extensively investigated [8-15]. Based on the thermal analysis of isothermal, adiabatic and polytropic processes, it was found that isothermal expansion in the engine had the largest power generation [2]. In reality, feasible solutions for expansion with approximate isothermal process in engine or turbine have been proposed. These include utilisation of ambient heat [8-11] and combination of ambient and combustion heat [12-13]. Manning et al [8] developed a direct drive system using multi-stage expansions with reheating prior to the final stage of expansion in Brayton cycle. A regenerative device was proposed to improve the heat efficiency. West et al. [9] used a double acting piston expander to improve the efficiency of the working fluid. For using environmental heat, Negre [10] (MDI company in France) firstly designed multistage engine system. Due to the utilisation of ambient heat, the expansion in the system was approximated to an isothermal process. Marquand [11] (University of Westminster) developed a two-stage turbine with a heat pipe before the inlet of engine to make use of environmental heat. The heat transfer area of the heat pipe was up to 1.4 m^2, while the heat transfer efficiency was 85%. It was reported that when the inlet pressure was 4.5 MPa, and engine speed was 1000 rpm, the power generation was as high as 25 kW.

In the above studies, the processes in engine were considered as multi-stage adiabatic expansion with middle reheating using the ambient heat. This is favourable for improving system efficiency and power generation by engine. However, since the inlet temperatures in the expansion stages of the engine were lower than ambient temperature, system efficiency and power capacity were significantly restrained. Oxley et al [12] utilized combined heat from both ambient and combustion in a Stirling engine. Oxygen from the liquefaction and separation of air was used to enhance the efficiency of fuel combustion. Latter et al [13] used liquid air as the working fluid in the Rankine cycle. They utilized ambient heat to increase the liquid air temperature in the multi-stage expansion process. Additional fuel was subsequently injected to make use of the combustion heat in an internal combustion engine. Comparing with no utilisation of combustion heat, it was reported that the power generation increased by 50%.

Apart from utilisation of environmental heat and combustion heat during the multi-stage expansion processes, other methods for improving system efficiency and power generation include controlling of injecting time of high pressure gas [10] and parametric optimization of engine [14-15]. Negre et al [10] developed an engine system, with high pressure gas injected into the engine intermittently. In the system, air was absorbed into the chamber of engine when the piston went down from top dead centre (TDC) to bottom dead centre (BDC). The absorbed air was then compressed to 20 bar under 400 ^{o}C in the movement of piston in the BDC to TDC process, during which the high pressure gas was injected. As a result, the temperature of the mixture (expansion gas and the high pressure air) was improved, leading to an increased power generation by the engine. However, due to the short injecting time, the thermal energy from the high pressure gas was insufficiently absorbed in the mixing process. Consequently, Negre [10] designed a special crank published in patent to control time for mixture. With the new connecting rod, the piston can stay near the top for about 70^{o} of the

shaft rotating. As a result, the components from two different injections are fully mixed, leading to a largely improved power capacity of the engine system.

Group of Knowlend in University of Washington has done lots of work on parametric optimization of engines. As claimed by Knowlend et al [14], parametric optimization of engine was also feasible for improving power generation under the same conditions. Small radius of chamber, long length of stroke and low engine speed were all favourable for improving power generation and system efficiency of the engine. Knowlend et al [14] also designed jagged surfaces for both cylinder block and piston with heater core imbedded inside expansion chamber. In the design, heat transfer agent was used to increase temperature of HTF. Knowlend et al [15] analyzed the enhancement of heat transfer rate by this novel piston-head configuration. They claimed that by imbedding a heater core within the expansion chamber, the expansion efficiency in the engine was performed as 85% of the ideal isothermal process.

With a new valve scheme connected, a piston based engine system was developed in this study. By setting an optimal p-crank angle, the maximum power generation rate through gas expansion in the engine chamber can be achieved. The power generation of the piston based engine was estimated by establishing a theoretical model. Parameters effects, promotion of power capacity, engine efficiency and its effect on the CES efficiency were investigated.

2. An engine system for cold to power conversion

Cold energy storage technology stores off-time electricity as cold energy in the cold storage media and regenerates electricity in engine/ turbine system by utilising the cold exergy through thermodynamic cycle [16]. A regenerator was used in the Rankine cycle for improving the efficiency of the thermal dynamic cycle and the CES system. Figure 1 showed the role of engine in the CES system, and a specific piston based engine system used for

power/ electricity generation. The referred engine system was mainly composed by an engine, a motor/ electrical generator and a new valve scheme with associate controlling modules. The advantage of the engine system is the efficient controlling of the opening time of the engine inlet, by which high pressure and medium-to-high temperature gas was efficiently expanded.

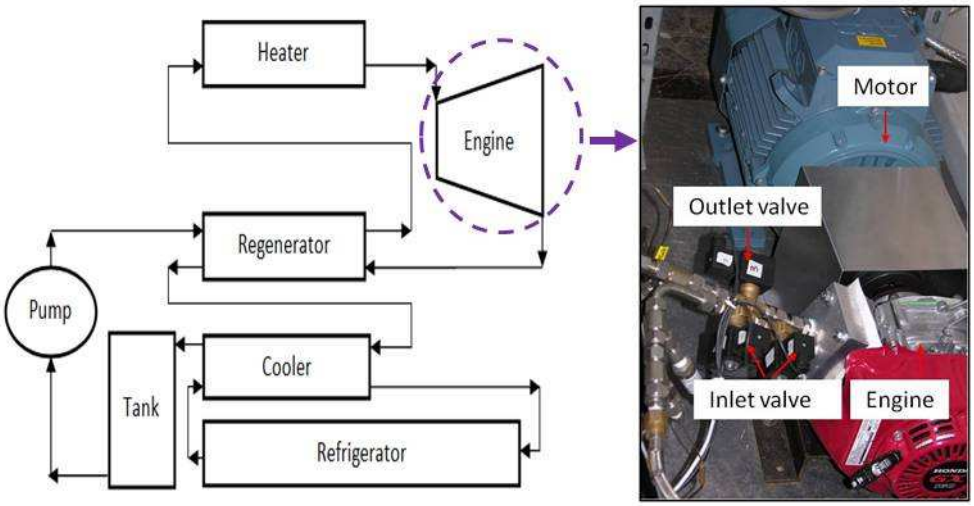

Figure 1. Schematic diagram of the experimental system.

Two solenoid valves were used at the inlet of the engine to control the opening time, since the expanding gas could only enter the chamber in the condition that two solenoid valves at the inlet were open simultaneously. For precisely controlling opening/ closing time of valves, count setting method was adopted. Specifically, the circle of the shaft in engine is equally divided into 320 parts. Each part is called one count. When the piston is at the top dead centre (TDC), an index is marked at the bottom of the shaft where the 0^{th} count is scheduled. In the controlling modules, opening and closing operations on valves are affected by the counts. The influence on valve operations is realized by initiating electrical voltage for all of the 320 counts in the circle of the shaft. Consequently, by resetting the electrical voltage on different counts, the opening and closing time for each valve can be controlled.

The piston based engine has two solenoid valves (V1, V2) installed at the inlet and another solenoid valve (V3) used at the outlet. The so-called p-crank angle is defined as the rotating angles of the shaft in a certain period when both valves at the engine inlet are open simultaneously. For instance, V2 is set open from 0^{th} count to 180^{th} count, while V2 is set open from 210^{th} count to 30^{th} count, as a result, the p-crank angle is $30\times\frac{360}{320}\approx 33.8^{o}$ (30 counts from 0^{th} count to 30^{th} count), as presented in Figure 2(a). In the opening time (t_1), piston moves from the TDC to the shown location (x); while at half periodic time ($t/2$), the piston reaches the bottom dead centre (BDC), as presented in Figure 2(b) where L is the length of the engine chamber.

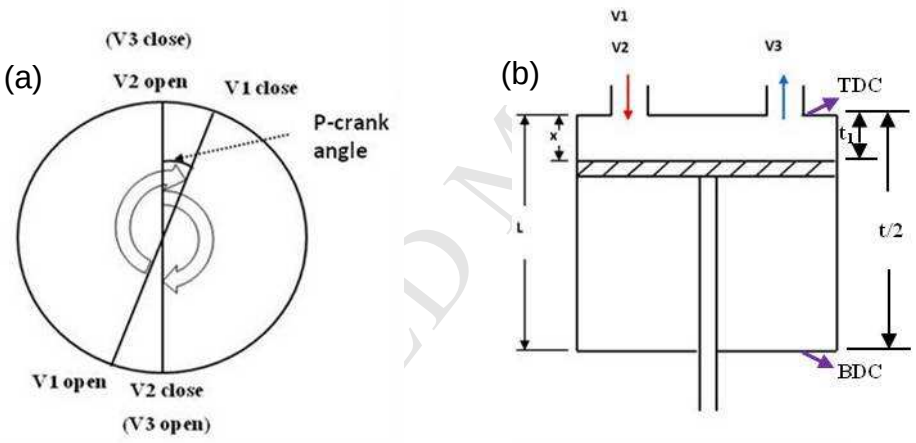

Figure 2. Details of the piston based engine: (a) formation of p-crank angle by count setting; (b) piston movement in the engine chamber.

For characterizing the p-crank angle, the opening time of the engine inlet is written as in Eq. (1):

$$\frac{t_1}{t/2}=\alpha \tag{1}$$

where α is the ratio of opening time to half periodic time of the engine. In this case, p-crank angle can be expressed as:

$$p-crank\ \ angle=180^{o}\cdot\alpha \tag{2}$$

In terms of Eqs. (1) ~ (2), it is seen that the increase of the p-crank angle results in the prolonging of the opening time of the valves. This indicates more mass flow rate (kg/s) of the expanding gas in the engine chamber. On the other hand, the expanding volume is reduced due to the continuous movement of the piston in the prolonged opening time, leading to a decreased specific power generation (J/kg). This indicates a significant effect of the p-crank angle on the power/ electricity generation rate (W) of the piston based engine system.

3. Theoretical model for predicting power generation by the engine

Thermal dynamic cycle of a piston based engine was demonstrated as process A-B-C-E, as presented in Figure.3. The process A-B is the gas injection into the engine chamber, during which mass of gas increases with time. The process B-C represents the expansion process. Since the valves at both inlet and outlet of the engine are closed, gas mass keep constant during the process. While the process C-E is the gas elimination process, when the gas mass in the chamber is reduced with time. One can see that there is no compression process for the engine driven by high pressure gas. As a result, the specific engine power (w, J/kg) is generated in the process B-C, which can be expressed as in Eq. (3):

$$w = \int_{P_B}^{P_C} -v \cdot dP \tag{3}$$

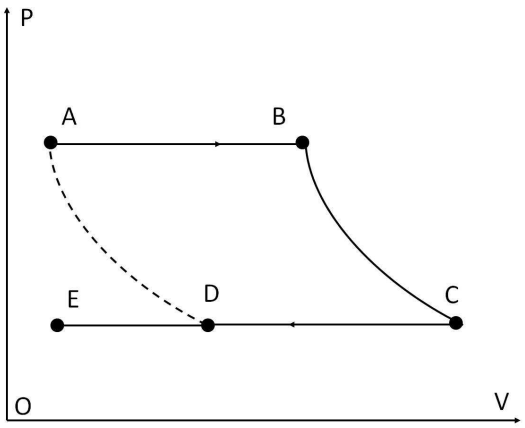

Figure 3. Thermal dynamic cycle in the piston based engine.

The gas expansion in the piston based engine can be either isothermal process or adiabatic process. As stated in [2], expansion in an isothermal process results in the maximum power output, compared with other thermal processes in the engine. However, the isothermal condition is difficult to be realized in practical engine tests, since the heat transfer process between the expanding gas (i.e. CO_2 or air) and the ambient is inefficient in a short time. With a high motor speed (i.e. 2900 rpm), little amount of heat can be transferred to the ambient. In this regard, gas expansion (process B-C) can be considered as the adiabatic expanding process, which is analysed in the following.

3.1. Specific power

Although the expanding process in the engine is irreversible due to the pressure difference between the chamber and the ambient, it is regarded as approximate adiabatic process due to the prompt expanding of gas in the chamber. Consequently, the process equation can be written as:

$$P_B v_B^{\,k_{po}} = P_C v_C^{\,k_{po}} \tag{4}$$

where k_{po} is the Possion factor, which is defined as,

$$k_{po} = \frac{C_{p,g}}{C_{V,g}} \tag{5}$$

in which $C_{p,g}$, $C_{V,g}$ are the heat capacity of gas at constant pressure and volume, respectively. The technical power by the engine can be expressed as:

$$w = \int_{P_{x=x}}^{P_{x=L}} -v \cdot dP \tag{6}$$

From Eqs. (4)~(6), the specific power generation in the adiabatic process of an ideal gas is calculated as:

$$w = \frac{1}{k_{po} - 1} \cdot R_g \cdot T_{in} \cdot [1 - (\frac{P_c}{P_{in}})^{\frac{k_{po}-1}{k_{po}}}] \quad (7)$$

In which R_g is the gas constant ($J/(kg \cdot K)$); P_{in} and T_{in} are pressure and temperature of the expanding gas at the inlet of the piston based engine, respectively; P_c represents the gas pressure after expansion when the piston reaches the BDC of the chamber. In ideal situation, P_c is equal to the ambient pressure ($P_c \approx P_o$). However, in the condition that the engine has an expansion ratio lower than P_{in} / P_c, P_c is higher than the ambient pressure, indicating a significant exergy loss in the expansion process.

3.2. Mass flow rate

Ideal-state equation for the expansion gas at the engine inlet is as below:

$$P_{in} \cdot V_g = m \cdot R_g \cdot T_{in} \quad (8)$$

Where m, V_g are the mass and volume of the expansion gas entering the engine chamber at the time t_1, respectively. Elhaj et al [17] developed a theoretical model for predicting the piston location during the rotation of the crankshaft. To characterize the movement of the piston, Figure 4 shows the schematic diagram of the connections between motor, the crankshaft and the piston of the engine.

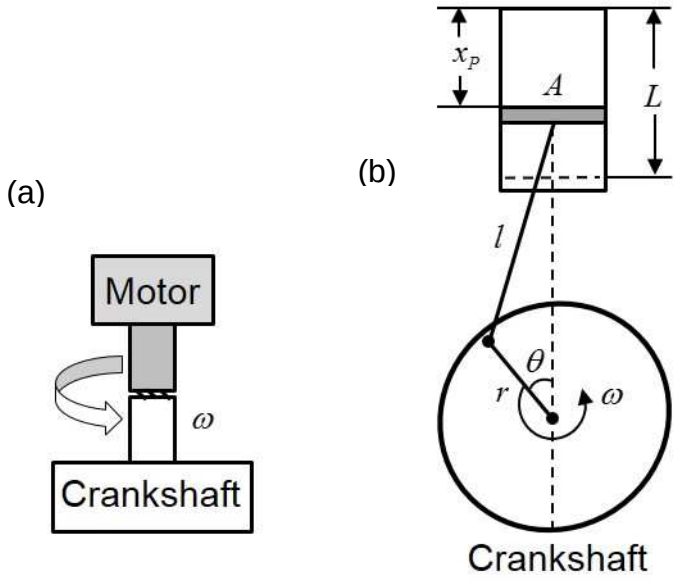

Figure 4. Schematic diagram of the motor and the piston based engine: (a) connection between motor and the crankshaft; (b) connection between the crankshaft and the piston.

Taking the TDC as the reference position, the piston location (x_P) can be formulated as the function of the rod length (l), crank radius (r) and the rotating angle (θ):

$$x_P = r(1-\cos\theta) + l[1-\sqrt{1-(\frac{r}{l})^2\sin^2\theta}] \tag{9}$$

Since the motor speed (ω) is controlled as constant values in the experimental system, the rotating angle can be written as:

$$\theta = \omega t \tag{10}$$

The volume of the gas in the engine chamber at the time t_1 can be expressed as:

$$V_g = x_P \cdot A \tag{11}$$

in which A is the sectional area of the engine chamber. In consideration of one rotation period (t), according to Eq. (8) ~ (11), the average mass flow rate ($\overline{\dot{m}}_{in}$) at the inlet is obtained:

$$\overline{\dot{m}}_{in} = \frac{m}{t} = \frac{P_{in}}{T_{in}} \cdot \frac{1}{2\pi R_g} \cdot \omega \cdot A \cdot \left\{ r[1-\cos(\omega t_1)] + l[1-\sqrt{1-(\frac{r}{l})^2\sin^2(\omega t_1)}] \right\} \tag{12}$$

Since it takes half of the rotation period for the piston moving from TDC to BDC, from Eq. (9), the relation of the crankshaft radius and the length of the engine chamber is established:

$$x_P = 2r = L \qquad (\text{when } \theta = \pi) \tag{13}$$

3.3. Power generation rate

The power generation rate of the piston based engine is calculated as the product of the specific power and the average mass flow rate. Therefore, based on Eq. (7) and Eq. (12), the average engine power rate can be calculated:

$$\overline{W} = \frac{1}{k_{po}-1} \cdot \frac{1}{2\pi} \cdot P_{in} \cdot \omega \cdot A \cdot [1-(\frac{P_c}{P_{in}})^{\frac{k_{po}-1}{k_{po}}}] \cdot \left\{ r[1-\cos(\omega t_1)] + l[1-\sqrt{1-(\frac{r}{l})^2 \sin^2(\omega t_1)}] \right\} \tag{14}$$

According to Eq. (1) and (2), the opening time (t_1) can be expressed as:

$$t_1 = \frac{p-crank\ \text{angle}}{180^o} \cdot \frac{\pi}{\omega} \tag{15}$$

The above analysis indicates that the average engine power rate is determined by the thermal physical parameters of the expansion gas (i.e. pressure and Possion factor), geometric parameters (i.e. the volume, sectional area and length of the chamber, the rod length, and the crank radius) and the operating conditions including the p-crank angle, the expansion ratio and the motor rotating speed. However, since P_c is affected by the key parameters such as the p-crank angle, rotating speed and the chamber volume, optimal parameters exist for achieving the maximum power generation by the engine.

In the practical engine system, the valves installed at the inlet and outlet of the engine has their minimum inner diameters. For example, for small valve that has a reflection time of 15ms for opening and closing operations, the minimum inner diameter (D_v) is 1.8 mm. Due to the gas flowing velocity in the valve is restrained below the sound velocity ($u_m = 340 m/s$), the volume flow rate at the inlet of the piston based engine becomes a limited value (

$\bar{\dot{V}}_{in} \le \frac{\pi}{4} D_v^{\,2} \cdot u_m$). In the period that the piston moves from the TDC to the BDC, the average volume flow rate can be written as:

$$\bar{\dot{V}}_{in} = \frac{1}{\pi} \cdot \omega \cdot A \cdot \left\{ r[1-\cos(\omega t_1)] + l[1-\sqrt{1-(\frac{r}{l})^2 \sin^2(\omega t_1)}] \right\} \quad (16)$$

Based on the above equations, the maximum rotating speed is evaluated as 160 rpm. This indicates that the power generation rate is affected by the motor rotating speed when it is less than the maximum value (160 rpm). However, due to the limitation of the volume flow rate of the expansion gas, the power generation rate is not significantly influenced with further increasing of the rotating speed. Figure 5 was the experimental results showing the effect of motor speed on the engine power generation. In the figure, EP (written as Pow_2) represented the contribution of the engine for power production, EC (written as Pow_1) was the electricity consumption, while EM (written as $Pow_1 - Pow_2$) was the net electricity output of the system. It was shown that although there was small fluctuation under a motor speed beyond 160 rpm, the power generation by engine (EP) became approximately stable.

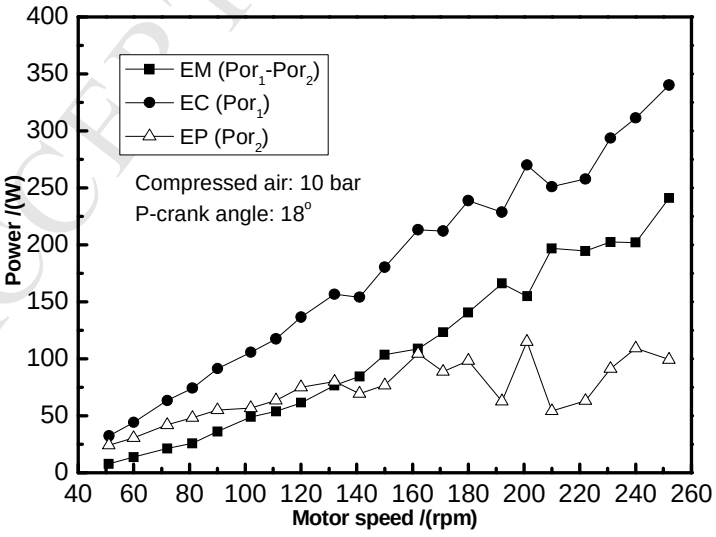

Figure 5. Effect of the motor speed (with small valves).

4. Optimal p-crank angle

As aforementioned, the optimal p-crank angle exists since the mass flow rate of the expansion gas increases while the specific power generation is reduced with increasing of the p-crank angle. For the gas expansion process, ideal-gas equation can be described as Eqs.(17)~(18):

$$P_{in}x^{k} = P_{c}L^{k} \tag{17}$$

$$\frac{x}{L} = (\frac{P_{c}}{P_{in}})^{\frac{1}{k}} \tag{18}$$

In terms of Eq. (14), (17) and (18), the average power rate of the piston based engine can be written as:

$$\overline{W} = \frac{1}{k_{po}-1}\cdot\frac{1}{2\pi}\cdot P_{in}\cdot\omega\cdot A\cdot[1-f(\theta)^{(k_{po}-1)}]\cdot f(\theta)\cdot 2r \tag{19}$$

In which,

$$f(\theta) = \frac{r[1-\cos(\theta)]+l[1-\sqrt{1-(\frac{r}{l})^{2}\sin^{2}(\theta)}]}{2r} \quad (\theta = \pi\alpha) \tag{20}$$

For achieving the maximum power rate, the following equations are resulted:

$$\left\{f(\theta)\cdot[1-f(\theta)^{(k_{po}-1)}]\right\}' = 0 \tag{21}$$

$$f(\theta) = k_{po}^{-\frac{1}{k_{po}-1}} \tag{22}$$

As a result, the optimal p-crank angle is obtained. In a case study, the radius of the crankshaft is the same as the length of the rod ($r = l$), consequently,

$$\theta = \arccos[1-k_{po}^{-\frac{1}{k_{po}-1}}] \quad \text{(in Rad)} \tag{23a}$$

$$\alpha = \frac{\arccos[1-k_{po}^{-\frac{1}{k_{po}-1}}]}{\pi} \tag{23b}$$

$$p-crank\ \text{angle} = \frac{180}{\pi}\arccos[1-k_{po}^{-\frac{1}{k_{po}-1}}] \quad \text{(in Degree)} \tag{23c}$$

For compressed air under different temperatures, the Possion factor k_{po} is in the range of 1.2~1.4. According to the above equations, the optimal p-crank angle in the case study is calculated as approximately 55^o. The value of α is evaluated as around 0.307, indicating the opening time represents 15.4% of the motor rotation period for achieving the maximum power rate of the piston based engine. The case study also shows that the ratio of the piston location to the chamber length is 42.7% by the end of the opening time. This allows the gas to be expanded with the maximum mean power rate.

Figure 6 shows the influence of the length ratio of the rod to the crankshaft (L/r) on the optimal p-crank angle. The figure indicates that the optimal p-crank angle increases from approximately 55^o to 76^o with a variation of the length ratio from 1 to 5. Furthermore, with the expansion gas that has a higher Possion factor, the p-crank angle for achieving the maximum power generation by the engine is normally 1^o~4^o larger.

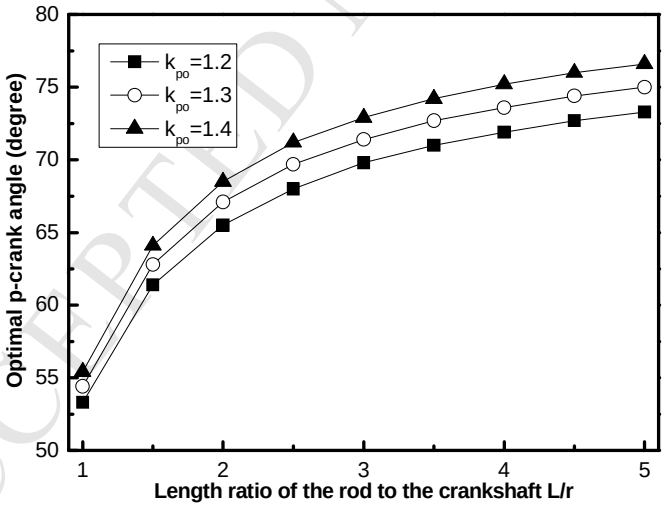

Figure 6. Variation of the optimal p-crank angle due to the change of the length ratio of the rod to the crankshaft.

The effect of the p-crank angle on the power generation by the engine is shown in Figure 7. With the increase of the p-crank angle, the power contribution by the engine increases firstly and decreases subsequently. The highest power by engine is obtained under the optimum p-

crank angle. It is shown that under different Possion factor, the optimum p-crank angle is slightly changed.

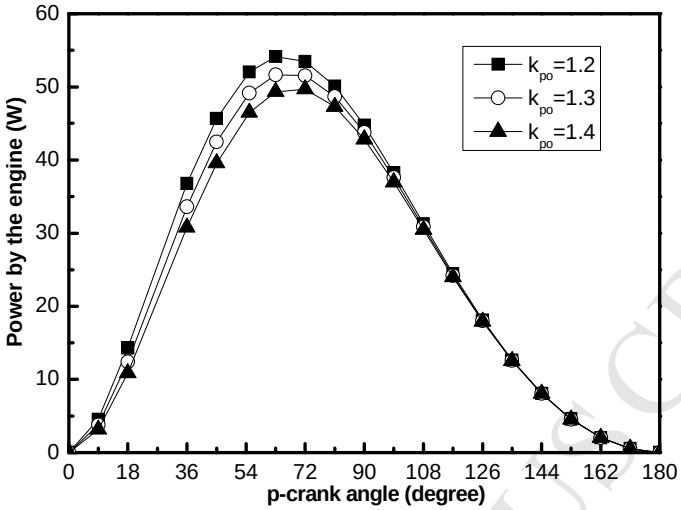

Figure 7. The effect of p-crank angle on the engine power generation (compressed air: 10 bar; motor speed: 60 rpm).

5. Power capacity of the engine under high operating parameters

This section aims to estimate the power capacity of the piston based engine under different operating parameters, including the motor speed, gas pressure and temperature. The parametric study was conducted under the optimal p-crank angle for obtaining the maximum power generation in theory. Figure 8 shows the effect of motor speed in the condition of providing compressed air to a small engine (with a chamber volume of 162 cm^3) for expansion. When motor speed was lower than160 rpm, the power generation by engine increased linearly with increasing of the motor speed. However, due to the restriction by the smallest section area of the flowing passage in the valves, the power generation became constant with a motor speed beyond 160 rpm.

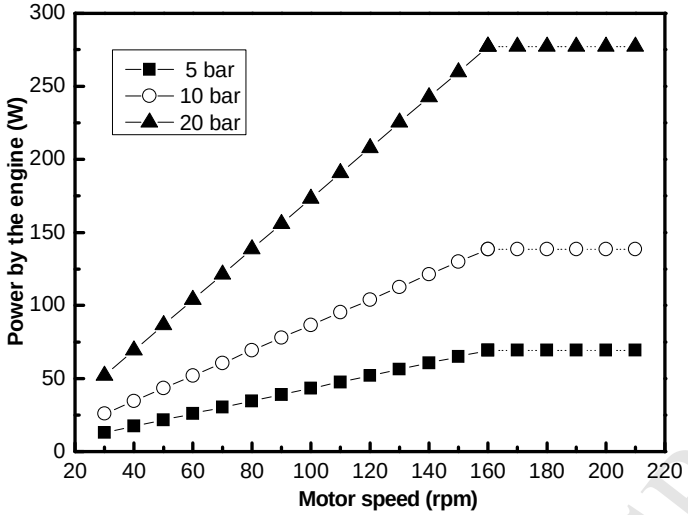

293

294 Figure 8. Effect of the motor speed on the power generation by the small engine.

295 Figure 9 and Figure 10 presents the effects of pressure and temperature on the power
296 capacity of the small engine (chamber volume of 162 cm^3), respectively. As can be seen in
297 Figure 9, power generation increased linearly with the increase of the gas pressure. It was
298 noted that the positive effect of gas pressure on promotion of the power generation became
299 more significant under a relatively higher motor speed (within 160 rpm). However, the effect
300 of the gas temperature was featured differently with changed provision of the expansion gas
301 to the engine. Figure 10 indicated the temperature influence was not obvious. This is because
302 the multiplier $[1-(\frac{P_c}{P_{in}})^{\frac{k_{po}-1}{k_{po}}}]$ in Eq. (14) is relatively small for the expansion gas with a
303 temperature in the range of 300~1000 K. Compared with the compressed air, CO_2 led to more
304 power generation by the engine. Consequently, CO_2 is regarded as a better option as the
305 expansion gas in the engine for power generation.

306

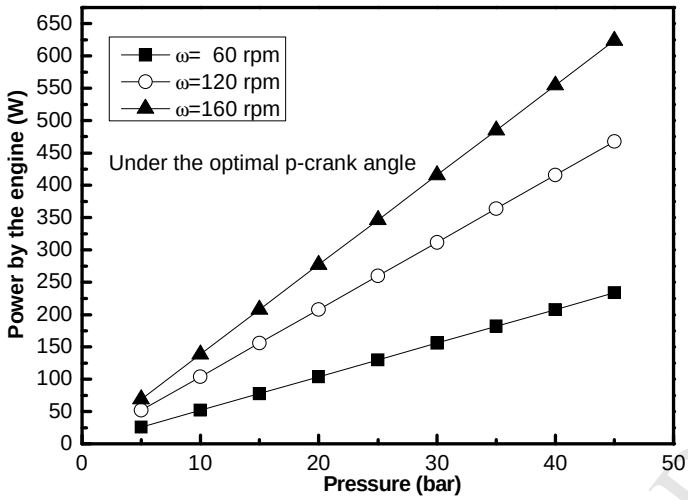

307

308 Figure 9. Effect of the gas pressure on the power generation by engine.

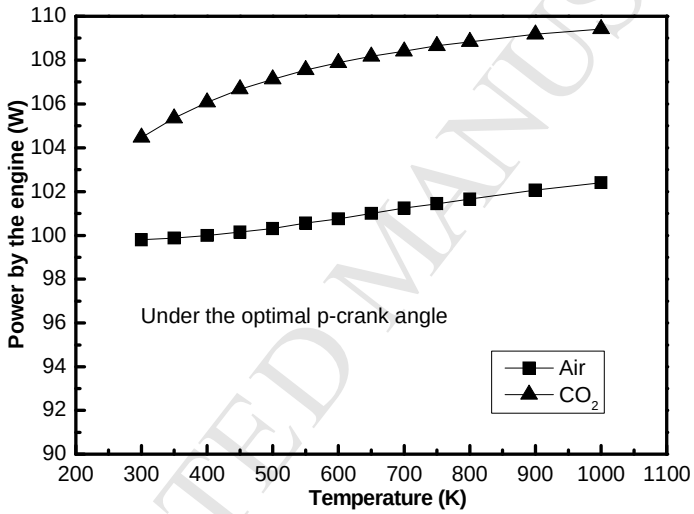

309

310 Figure 10. Effect of the gas temperature on the engine power generation.

311 As mentioned in the above section, power generation by the piston based engine is
312 restricted by the minimum inner diameter of the valves. Theoretically, the velocity of gas is
313 less than the sound velocity 340 m/s. As a result, the critical motor speed (ω_{cr}) is induced,
314 which indicates the maximum power capacity of engine under certain parameters:

315 $$\omega_{cr} = \frac{\pi^2}{4} \cdot \frac{340 D^2_{v,\min}}{V} \quad (24)$$

316 Figure 11 shows the calculated critical motor speed for different volume engines with a given
317 $D_{v,\min}$. In the case studies in which valves with the minimum diameter of 1.8 mm and 12 mm

318 are used, the critical motor speed is estimated as approximately 160 rpm and 600 rpm,
319 respectively. Since high motor speed results in large power generation by the engine, large
320 valves with increased $D_{v,\min}$ is suggested to be used for enlarging the power capacity of the
321 engine system.

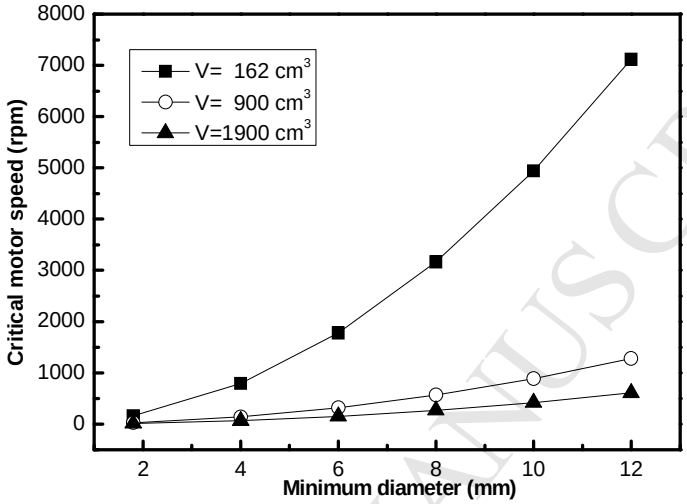

322

323 Figure 11. The critical motor speed affected by the minimum diameter of the valve and the
324 engine volume.

325 The power capacity of the large engine (1900 cm^3) using large valves ($D_{v,\min}$ =12 mm) was
326 predicted, as shown in Figure 12. Compressed air with pressure of 5, 10 and 20 *bar* was
327 expanded in the engine respectively. It was found that the maximum power generations at the
328 motor speed of 600 rpm in the above cases were as high as 3 kW , 6 kW and 12 kW ,
329 respectively. Beyond the motor speed of 600 rpm, the power generation was restrained by the
330 fixed $D_{v,\min}$ of the valves. With larger valves used, improved maximum power by the engine
331 can be achieved under a higher critical motor speed (>600 rpm). However, the large time
332 delay of the large valves may cause failure in controlling the opening and closing operations
333 under high motor speed.

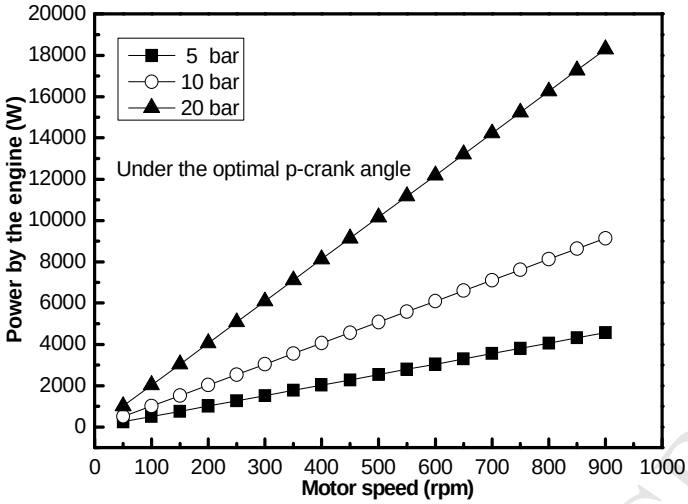

Figure 12. The prediction of power capacity of the large engine (1900 cm^3).

6. Further discussions on the piston based engine

In theory, the power generation by the engine is affected by the p-crank angle, motor speed, gas pressure and temperature, chamber volume and the minimum inner diameter of the valves used at the inlet and outlet of the piston based engine. However, in practical cases, the engine power generation is also significantly influenced by the performance of engine in the gas expansion process. This section concerns the efficiency of the engine and its effect on the energy storage efficiency of the CES system.

6.1 Engine efficiency

The engine efficiency refers to the exergy efficiency that is defined as the ratio of actual power output to the theoretical engine power based on the thermal analysis. In the case study of the small engine (162 cm^3), the practical power generation by experiments was expressed as $36.2\times Tor_2\cdot\omega$, where ω is the motor speed, while Tor_2 represented the torque percentage by engine contribution. Consequently, the engine efficiency can be formulated:

$$\eta_{engine}=\frac{36.2\times Tor_2\cdot\omega}{\frac{1}{k_{po}-1}\cdot\frac{1}{\pi}\cdot P_{in}\cdot\omega\cdot A\cdot[1-(\frac{P_c}{P_{in}})^{\frac{k_{po}-1}{k_{po}}}]\cdot\left\{r[1-\cos(\omega t_1)]+l[1-\sqrt{1-(\frac{r}{l})^2\sin^2(\omega t_1)}]\right\}} \quad (25a)$$

In the experiments, electricity consumption (EC) and electricity output on the motor (EM) were measured, therefore, the engine efficiency can be expresses as:

$$\eta_{engine} = \frac{EC - EM}{\frac{1}{k_{po}-1}\cdot\frac{1}{\pi}\cdot P_{in}\cdot\omega\cdot A\cdot[1-(\frac{P_c}{P_{in}})^{\frac{k_{po}-1}{k_{po}}}]\cdot\left\{r[1-\cos(\omega t_1)]+l[1-\sqrt{1-(\frac{r}{l})^2\sin^2(\omega t_1)}]\right\}} \quad (25b)$$

In a case study with a large engine (1900 cm^3), the inlet pressure of the compressed air was 20 bar, the inlet angle was set as 18^o while the motor speed was 60 rpm. The measured electricity consumption (EC) on the motor was 60 W, while the maximum net electricity output of the motor (EM) was -160 W. Therefore, the engine power (EP=EC-EM) generation was as high as 220 W. Based on the given parameters in the case study, the theoretical engine power was evaluated as 664 W. According to Eq.(25), the engine efficiency for the large engine under the conditions was approximately 33.1%. For a small engine (162 cm^3) under the same operating conditions, EC and EM were measured as 45 W and 15 W, respectively. As a result, the engine power (EP) was equal to 30 W. However, the theoretical engine power was calculated as 57 W under the conditions, so the engine efficiency of the small engine was as high as 52.6%. It was noted that the large engine induced a lower engine efficiency. This is because more exergy loss is caused due to the inadequate gas expansion in the large engine chamber. However, it doesn't indicate small engine is better, since the engine system results in a net electricity consumption (EM) indicating the non-feasibility of the engine in a real CES system.

6.2 Influence of the engine efficiency on energy storage efficiency

Although the efficiency of the large engine is relatively lower than that of the small engine, large engine is still recommended to be used in a CES system. This is because large engine

can result in a net power generation that can be sent back to the electrical grid for peaking shifting purpose.

From the point of view of energy storage and utilisation, the contribution of the engine system lies in the net output power by the system. Therefore, the actual engine efficiency can be expressed as:

$$\eta'_{engine} = \frac{-EM}{\frac{1}{k_{po}-1}\cdot\frac{1}{\pi}\cdot P_{in}\cdot\omega\cdot A\cdot[1-(\frac{P_c}{P_{in}})^{\frac{k_{po}-1}{k_{po}}}]\cdot\left\{r[1-\cos(\omega t_1)]+l[1-\sqrt{1-(\frac{r}{l})^2\sin^2(\omega t_1)}]\right\}} \quad (26)$$

As a result, in the above case study, the large engine system had an actual efficiency of 24.1%. In contrast, for the small engine system, the actual engine efficiency for power generation was -26.3%.

In the CES system as demonstrated in [2, 16], the energy storage efficiency of the CES system can be formulated as:

$$\eta_{CES} = \frac{W_e - W_p}{E_{heat} + E_{cold}} \quad (27)$$

where W_e represents the power generation by the engine system; W_p is the electricity consumption for pumping the working fluid in the Rankine cycle; E_{cold} represents the electricity consumption for storing cold energy in the cold storage media; E_{heat} is the electricity consumption by heaters in the Rankine cycle. From the above analysis, the storage efficiency is written as:

$$\eta_{CES} = \frac{-EM - W_p}{E_{heat} + E_{cold}} \quad (28)$$

A case study was presented below to show the influence of the actual engine efficiency on the energy storage efficiency of the CES system. In the case study, the expansion gas was

heated up to 200 ^{o}C by the heater in the Rankine cycle. Since pump was not used in the actual operation, the electricity consumption by the pump was zero. With a mass flow rate of 0.0426 kg/s, the theoretical engine power was:

$$EP_{theo} = 0.0426 \times \frac{1}{k_{po} - 1} \cdot R_g \cdot T_{in} \cdot [1 - (\frac{P_c}{P_{in}})^{\frac{k_{po}-1}{k_{po}}}] \quad (29)$$

which was calculated as 8659 W under the above operating conditions. In terms of the above engine efficiency of 33.1%, the actual engine power (EP) by the large engine was 2866 W. However, in consideration of the electricity consumption (EC) by the system, the net output of the engine system was further reduced to 2084 W. In the experiment, the electricity consumption by the refrigerator (E_{cold}) for cold energy storage was 4000 W, while the electricity consumption in the super heater (E_{heat}) for heating the working fluid to 200 ^{o}C was 7000 W (electricity consumed) or 0 W (waste heat from diesel engine used). As a result, the CES efficiency was estimated as approximately 18.9% and 52.1%, respectively. This indicates that for storing 10 kW of cold energy by consuming cheap electricity in off-peak time, the CES system has a capacity of feeding back electricity of 1.9~5.2 kW that can be later used in peak time. Therefore, engine efficiency in practical operations is still a big challenge for promoting the CES technology development.

7. Concluding remarks

Theoretical study indicates the significant effect of p-crank angle on the power generation by a piston based engine. Under different operating conditions and the geometric parameters of the engine (i.e. the length ratio L/r), the optimal p-crank angle which leads to the maximum power generation varies in the range of 55^{o} and 76^{o}. Apart from that, motor speed, gas pressure and temperature, and chamber volume have positive influence in increasing the power generation by the piston based engine. However, the promotion of the power capacity

is limited by the minimum inner diameter of the valves at both inlet and outlet of the engine system.

Although large engines have a lower engine efficiency compared with small engines due to the more exergy loss in the chamber, it is still competitive since a net power generation is induced, showing its feasibility in a real CES system. Considering the power consumptions by the motor, the actual efficiency of the large engine was calculated as 24.1% in a case study, while in contrast, it was -26.3% for the small engine in the case. Due to the low engine efficiency, the energy storage efficiency of the CES system in two different situations was estimated as approximately 18.9% (when electricity consumed in the super heater) and 52.1% (when waste heat from diesel engine is recovered), respectively. Therefore, there is a long way for improving the engine performance. However, from the point of view of electricity saving in off-peak time, cold energy storage is still worthwhile.

Acknowledgement

We would like to acknowledge EPSRC Grants (EP/L014211/1, EP/K002252/1 and EP/L019469/1) for financial support.

References

[1] Qureshi WA, Nair NK, Farid MM. Impact of energy storage in buildings on electricity demand side management. Energy Conversion and Management 2011, 52(5): 2110-2120.

[2] Du Y P. Cold energy storage: fundamentals and applications. PhD thesis, 2014.

[3] IEEJ-The institute of energy economics, Japan, 2005.

[4] Oren S. Capacity Payments and Supply Adequacy in a Competitive Electricity Market. University of California at Berkeley.

[5] Swider DJ. Compressed air energy storage in an electricity system with significant wind power generation. IEEE Transactions on energy conversion 2007, 22(1):95-102.

[6] Lane GA. Solar heat storage—latent heat materials. vol. I. Boca Raton, FL: CRC Press, Inc, 1983.

[7] Du Y P, Ding Y L. Feasibility of small-scale cold energy storage (CES) through carbon dioxide based Rankine cycle. Journal of Energy Storage 2016; 6: 40-49.

[8] Manning L, Schneider RN: Nitrogen Vapor Engine. Patent No. 3,786,631, Jan. 22, 1974.

[9] West CW, Lee LE, Norris AO: Vehicle Utilizing Cryogen fuel. Patent No. 4,106,581, Aug.15, 1978.

[10] http://www.theaircar.com/

[11] http://freeenergy.co.za

[12] Oxley AJ: Methods and Means for Storing Energy. Patent No. 4,227,374, Oct. 14, 1980.

[13] Latter AL, Dooley JL, Hammond RP: Engine System Using Liquid Air and Combustible Fuel. Patent No. 4,359,118, Nov. 16, 1982.

[14] Williams J, Knowlen C, Mattick AT, Hertzberg A: Frost-Free Cryogenic Heat Exchangers for Automotive Propulsion. AIAA 97-3168.

[15] Knowlen C, Williams J, Mattick AT, Deparis H, Hertzberg A: Quasi-isothermal expansion engines for liquid nitrogen automotive propulsion. SAE 972649, 1997.

[16] Du Y P, Ding Y L. Optimization of cold storage efficiency in a Rankine-cycle based cold energy storage system. Energy Technology, 2016.

[17] Elhaj M, Gu F, Ball A D, Albarbar A, Al-Qattan M, Naid A. Numerical simulation and experimental study of a two-stage reciprocating compressor for condition monitoring. Mechanical Systems and Signal Processing 2008; 22: 374-389.

Address: CSIRO Manufacturing Flagship, Gate 3 Normanby Rd, Clayton, VIC 3168, Australia
Postal Address: Private Bag 10, Clayton South, VIC 3169, Australia
• **ABN** 41 687 119 230

- Under different operating conditions and the geometric parameters of the engine (i.e. the length ratio L/r), the optimal p-crank angle which leads to the maximum power generation varies in the range of 55^{o} and 76^{o}.
- Although large engines have a lower engine efficiency compared with small engines due to more exergy loss in the chamber, it is still competitive since a net power generation is induced, showing its feasibility in a real CES system. Considering the power consumptions by the motor, the actual efficiency of the large engine was calculated as 24.1% in a case study, while in contrast, it was -23.6% for the small engine in the case. Due to the low engine efficiency, the energy storage efficiency of the CES system was estimated as 18.9% and 52.1% in two different situations.